Cell, Vol. 99, 589–601, December 10, 1999, Copyright ©1999 by Cell Press

Golgi Membranes Are Absorbed into and Reemerge from the ER during Mitosis

Kristien J. M. Zaal,* Carolyn L. Smith,§ Roman S. Polishchuk,‖ Nihal Altan,* Nelson B. Cole,* Jan Ellenberg,* Koret Hirschberg,* John F. Presley,* Theresa H. Roberts,* Eric Siggia,† Robert D. Phair,‡ and Jennifer Lippincott-Schwartz*#

*Cell Biology and Metabolism Branch
National Institute of Child Health and Human Development
National Institutes of Health
Bethesda, Maryland 20892-5430
†Center for Studies in Physics and Biology
Rockefeller University
New York, New York 10021
‡BioInformatics Services
Rockville, Maryland 20854
§Light Imaging Facility
National Institute of Neurological Disorders and Stroke
National Institutes of Health
Bethesda, Maryland 20892
‖Laboratory of Molecular Neurobiology
Consorzio "Mario Negri Sud"
66030 Santa Maria Imbaro
Italy

Summary

Quantitative imaging and photobleaching were used to measure ER/Golgi recycling of GFP-tagged Golgi proteins in interphase cells and to monitor the dissolution and reformation of the Golgi during mitosis. In interphase, recycling occurred every 1.5 hr, and blocking ER egress trapped cycling Golgi enzymes in the ER with loss of Golgi structure. In mitosis, when ER export stops, Golgi proteins redistributed into the ER as shown by quantitative imaging in vivo and immuno-EM. Comparison of the mobilities of Golgi proteins and lipids ruled out the persistence of a separate mitotic Golgi vesicle population and supported the idea that all Golgi components are absorbed into the ER. Moreover, reassembly of the Golgi complex after mitosis failed to occur when ER export was blocked. These results demonstrate that in mitosis the Golgi disperses and reforms through the intermediary of the ER, exploiting constitutive recycling pathways. They thus define a novel paradigm for Golgi genesis and inheritance.

Introduction

All membrane traveling from ER to plasma membrane passes through the Golgi complex, where proteins destined for the plasma membrane are separated from those to be retained in the ER/Golgi system. This function is carried out by membrane recycling pathways, both within the Golgi complex and back to the ER. Golgi to ER recycling is necessary for maintaining the surface area of the ER in the face of outward secretory traffic (Griffiths et al., 1984; Wieland et al., 1987), for ensuring that escaped ER proteins return to the ER (Pelham, 1995), and for the reutilization of membrane machinery involved in forward secretory traffic (Wooding and Pelham, 1998).

Golgi enzymes have traditionally been viewed as resident in the Golgi complex, since they are enriched in this compartment. However, these enzymes are highly mobile and undergo extensive recycling within Golgi stacks (Cole et al., 1996b; Harris and Waters, 1996; Love et al., 1998), and when ER export is blocked, they redistribute into the ER (Dascher and Balch, 1994; Cole et al., 1998; Storrie et al., 1998). These observations have led to the idea that Golgi enzymes are capable of recycling all the way back to the ER (Cole et al., 1996a, 1998; Storrie et al., 1998). The extent of such recycling has been assumed to be small (Brands et al., 1985). If large, return of Golgi components from the ER back to the Golgi could play a role in the regulation of Golgi structure, which reversibly disassembles during mitosis (Lucocq and Warren, 1987; Thyberg and Moskalewski, 1992) and in response to specific drugs (Lippincott-Schwartz et al., 1990; Lucocq, 1992; Takizawa et al., 1993).

In this study, we investigate the extent of Golgi protein cycling to the ER and its role in Golgi disassembly/reassembly in interphase and mitotic cells using green fluorescent protein (GFP) technology. Due to the properties of GFP, fusion proteins can be followed by time-lapse imaging, and they can be quantified and photobleached, allowing measurement of their lateral mobility and transport between compartments (Cole et al., 1996b; Sciaky et al., 1997; Hirschberg et al., 1998). By exploiting these techniques, we have found that Golgi proteins in interphase continuously transit between Golgi and ER membranes, so much so that perturbations that disrupt such cycling quickly lead to redistribution of Golgi proteins to the site of inhibition. Similarly in mitosis, when ER export stops, Golgi structure is lost as recycling Golgi proteins become trapped in the ER and is only regained when ER egress resumes at the end of mitosis. The finding that the ER plays an indispensable role as intermediate in the Golgi complex's life cycle in both interphase and mitosis represents a departure from previous models for Golgi maintenance and inheritance (Warren, 1993).

Results

GalTase-GFP, a Golgi Resident Protein, Resides in Both Golgi and ER Membranes at Steady State

If Golgi proteins undergo constitutive recycling to the ER, at any time a fraction of them should reside in the ER. To test this, we analyzed the steady-state distribution of the Golgi marker, galactosyltransferase tagged with GFP (GalTase-GFP; Sciaky et al., 1997), by quantitative imaging. The suitability of GalTase-GFP as a resident

#To whom correspondence should be addressed (e-mail: jlippin@helix.nih.gov).

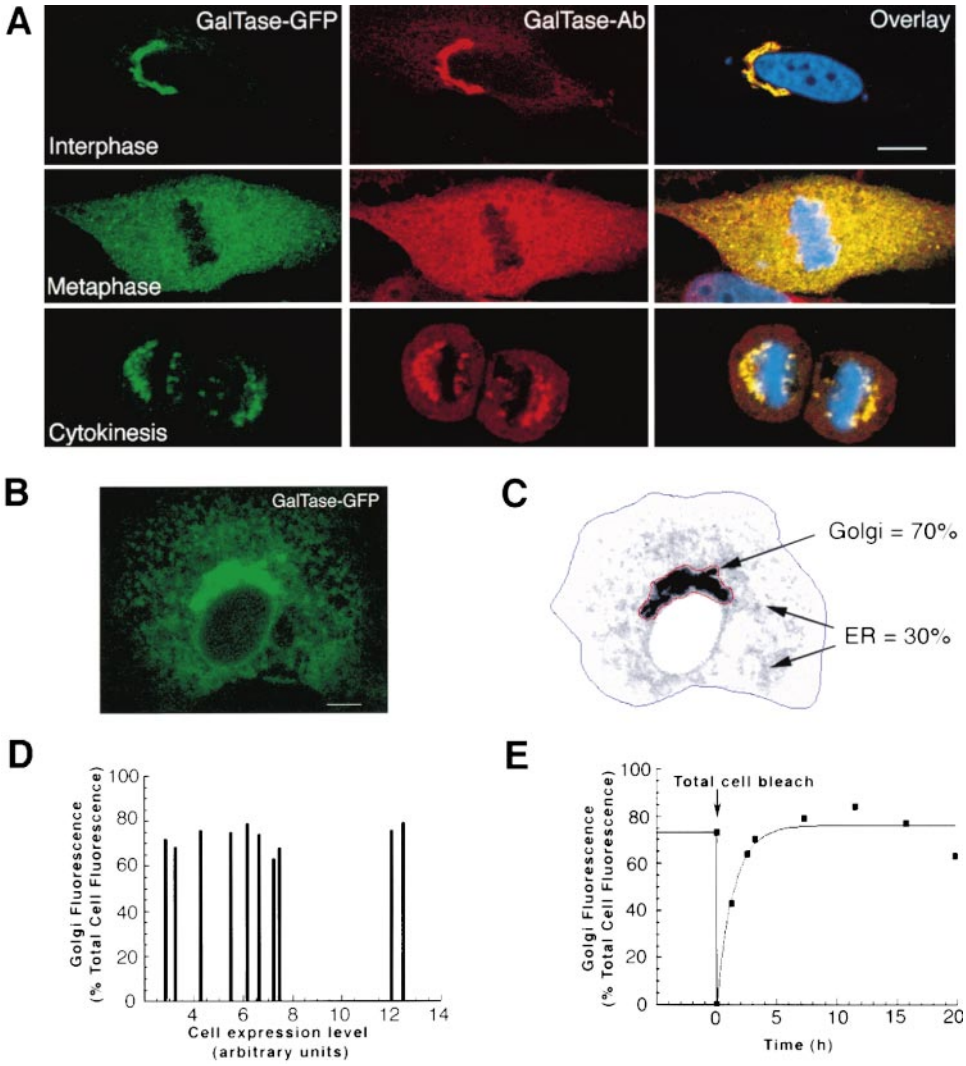

Figure 1. GalTase-GFP Colocalizes with Endogenous GalTase during All Stages of the Cell Cycle

(A) HeLa cells expressing GalTase-GFP were fixed and immunolabeled with antibodies that react with the endogenous GalTase, but not GalTase-GFP. The cells were counterstained with Hoechst dye for DNA (blue). GalTase-GFP (green) colocalized with endogenous GalTase (red) in cells in interphase, metaphase, and cytokinesis.

(B) In interphase cells, GalTase-GFP could be detected in the endoplasmic reticulum (ER) and nuclear envelope (which is continuous with the ER). The ER pool was visible in images collected with enhanced brightness.

(C) Quantitation of the two pools of GalTase-GFP showed that approximately 70% of the GalTase-GFP resided in the juxtanuclear Golgi complex and approximately 30% in the ER.

(D) The relative sizes of the two pools were similar in cells expressing different levels of GalTase-GFP.

(E) Newly synthesized GalTase-GFP assumes a steady-state distribution in the Golgi and ER over the course of several hours. A cell expressing GalTase-GFP at steady state was photobleached to remove all GFP fluorescence. Thereafter, the fluorescence in the Golgi and in the entire cell was measured at hourly intervals. Newly synthesized GalTase-GFP initially was concentrated in the ER (the site of synthesis). The steady-state distributions in the Golgi and ER were reestablished within approximately 5 hr. Bars, 10 μm.

Golgi marker was established previously by electron microscopy (Sciaky et al., 1997) and by colocalization at each stage of the cell cycle with endogenous GalTase (Figure 1A). In interphase HeLa cells, GalTase-GFP could be detected in the ER and nuclear envelope as well as in the Golgi complex (Figure 1B). The relative sizes of the Golgi and ER/nuclear envelope pools were estimated by measuring fluorescence intensities in the juxtanuclear Golgi compartment and the entire cell under appropriate detection parameters (Figure 1C). Approximately 70% of total fluorescence resided in Golgi membranes and 30% in ER membranes. Since the fluorescence from GalTase-GFP was equivalently detected regardless of its intracellular location, there are roughly 2.3× more GalTase-GFP molecules in Golgi than in ER membranes in these cells. Given that the surface area of the ER is at least 5-fold greater than that of the Golgi complex (Griffiths et al., 1984), this indicates that at steady state, GalTase-GFP is at least 15× more concentrated in Golgi membranes than in ER membranes.

The relative sizes of the Golgi and ER pools of GalTase-GFP were constant over time in interphase cells

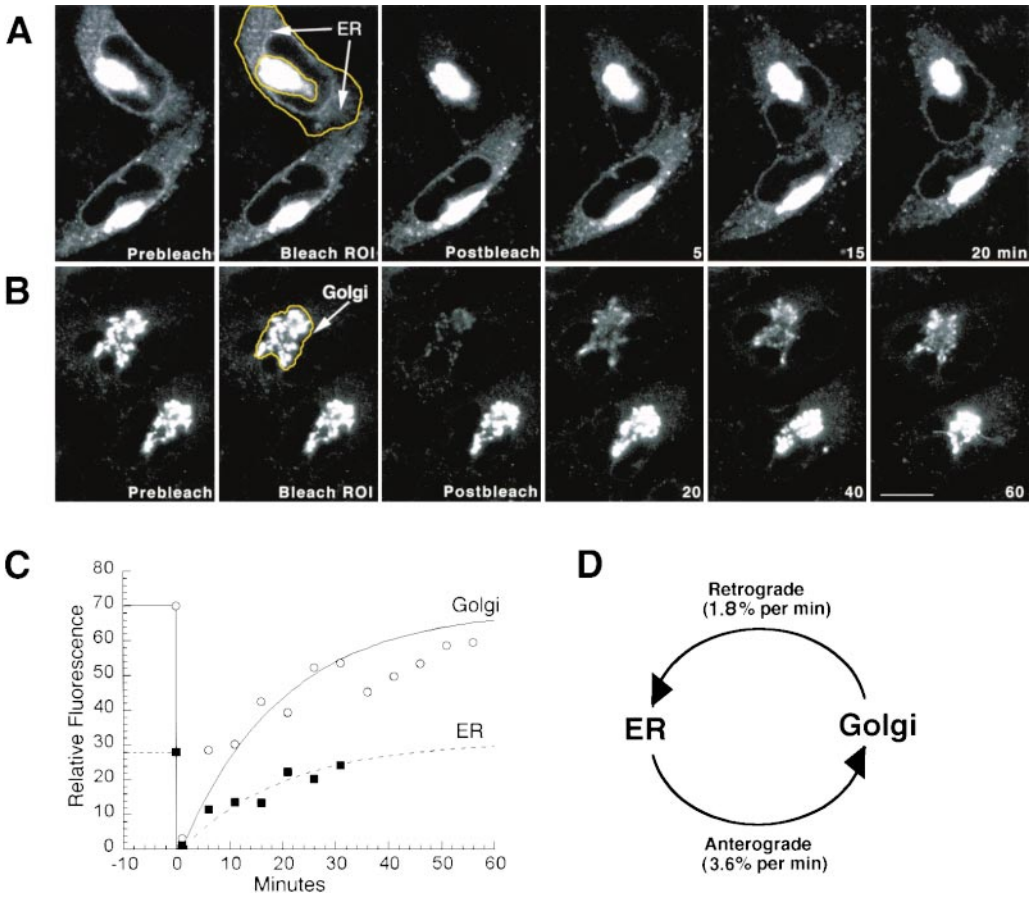

Figure 2. GalTase-GFP Continuously Cycles between the Golgi and ER in Interphase Cells

CHO cells stably expressing GalTase-GFP were incubated in 10 μg/ml cycloheximide 1 hr prior to and during the experiments to inhibit protein synthesis. In (A), the upper cell was photobleached within the outlined area (arrows) to remove fluorescence from the ER pool. Recovery was examined using imaging parameters appropriate for quantitating the pool of GalTase in the ER. In (B), the Golgi complex (outlined area) in the top cell was photobleached, and recovery was monitored using parameters appropriate for quantitating the fluorescence in the Golgi. Images at representative time points are shown (A and B). (C) Plots of the recovery of fluorescence into the photobleached areas in the experiments of (A) and (B) show that the ER (squares) and Golgi complex (circles) regained much of their prebleach fluorescence intensities (expressed as percentage of total cell fluorescence) within 30 min of bleaching. A two-compartment kinetic model, based on first order processes, was fit to the data (solid line for the Golgi, dashed line for the ER) to derive rate constants for anterograde and retrograde transport. The mean rate constants from five experiments were 3.6% per min for anterograde transport of GalTase-GFP and 1.8% per minute for retrograde transport (D).

and were independent of the expression level of GalTase-GFP (Figure 1D). Following photobleaching of the entire cell, GalTase-GFP fluorescence in the Golgi returned to 70% of total fluorescence after an initial lag and remained at this percentage as newly synthesized GalTase-GFP reequilibrated over ER and Golgi pools (Figure 1E). In other cell types, including CHO, NRK, COS, and PTK1, quantitation of GalTase-GFP fluorescence revealed a similarly fixed ratio of fluorescence between ER and Golgi pools (data not shown). These data suggest, therefore, that the ER pool of GalTase-GFP is not an artifact of overexpression, but together with the GalTase-GFP pool in Golgi membranes represents a steady state that cells actively maintain.

GalTase-GFP Constitutively Cycles between ER and Golgi Compartments

To investigate how the steady-state distribution of GalTase-GFP in Golgi and ER membranes arises and is maintained over time, we selectively photobleached Golgi or ER pools of GalTase-GFP and monitored recovery from the other pool in the absence of protein synthesis (Figures 2A–2C). Within 20 min of selectively photobleaching the ER pool of GalTase-GFP, ER membranes regained much the same percentage of total cellular fluorescence (i.e., about 30%) observed before bleaching (Figures 2A and 2C, squares). This was not due to synthesis of new GalTase-GFP, as evident from the lack of recovery of ER fluorescence in cycloheximide-treated cells that were completely bleached (data not shown). Moreover, after bleaching the ER pool selectively, Golgi-associated fluorescence decreased as fluorescence in the ER increased (data not shown). These results show that GalTase-GFP recycles from the Golgi complex along a retrograde pathway to the ER on a time scale of tens of minutes.

The ER pool of GalTase-GFP was similarly capable of exchanging with the Golgi pool; when the Golgi pool of

GalTase-GFP was selectively bleached (Figures 2B and 2C, circles), Golgi fluorescence began to recover within 20 min, and by 60 min had reached the same percentage of total cellular fluorescence (i.e., approximately 70%) observed before bleaching. The Golgi and ER, therefore, are capable of exchanging their GalTase-GFP pools without new protein synthesis.

Rate Constants for GalTase-GFP Cycling between Golgi and ER

Kinetic analysis from ER and Golgi photobleaching experiments permitted an estimation of the rate constants characterizing anterograde and retrograde transport of GalTase-GFP (Figures 2C and 2D). Standard methods of kinetic analysis were used, with the ER and Golgi pools of GalTase-GFP treated as two compartments exchanging via first order processes, each with a characteristic rate constant. The Golgi (or ER) fluorescence was fitted to the transient solution produced by this two-compartment model when the fluorescence in that compartment was suddenly set to zero and allowed to return to its original steady state (Figure 2C). The model solution (Figure 2D) predicted transport of GalTase-GFP in the anterograde (ER-to-Golgi) direction at a rate of 3.6% $\pm$ 0.17% of ER content per minute. Retrograde (Golgi-to-ER) transport was slower (in keeping with the steady-state distribution of GalTase-GFP); only 1.8% $\pm$ 0.37% of Golgi-associated GalTase-GFP returns to the ER per minute. These rate constants translate to mean GalTase-GFP residence times of 27.5 $\pm$ 1.2 min in the ER and 57.2 $\pm$ 11.3 min in the Golgi, yielding a mean cycle time of 84.6 $\pm$ 11.3 min.

Golgi Dissolution and Remodeling in Response to Perturbations in ER/Golgi Cycling Pathways

ER export is known to be inhibited without effects on retrograde traffic in cells expressing a predominantly GDP-bound mutant of Sar1p (mSar1p; Barlowe et al., 1994; Kuge et al., 1994; Shima et al., 1998). We found that GalTase, as well as other Golgi enzymes, were trapped in the ER and that Golgi structures were absent within a few hours of microinjection of cells with high concentrations of mSar1p plasmid (Figure 3A). The rate at which Golgi proteins appeared in the ER under these conditions was too fast to be explained solely by trapping of newly synthesized Golgi enzymes, since over 20 hr is required for GalTase-GFP fluorescence to be replenished through synthesis (data not shown). To verify the ER localization of the Golgi enzymes in mSar1p-expressing cells, we looked for modifications of ER resident glycoproteins by redistributed Golgi enzymes (Figure 3B). In untreated cells, Tac-E19 is sensitive to endoH throughout its lifetime, indicating that the steady-state pools of Golgi enzymes residing in the ER are normally insufficient to catalyze the multiple steps of processing required for conversion of oligosaccharides to endoH resistance (Hsu et al., 1992). In cells overexpressing mSar1p, however, Tac-E19 became endoH resistant. A similar effect has been observed in cells treated with BFA, a drug that induces retrograde transport of Golgi enzymes into the ER (Lippincott-Schwartz et al., 1990). These results indicate that Golgi enzymes redistribute

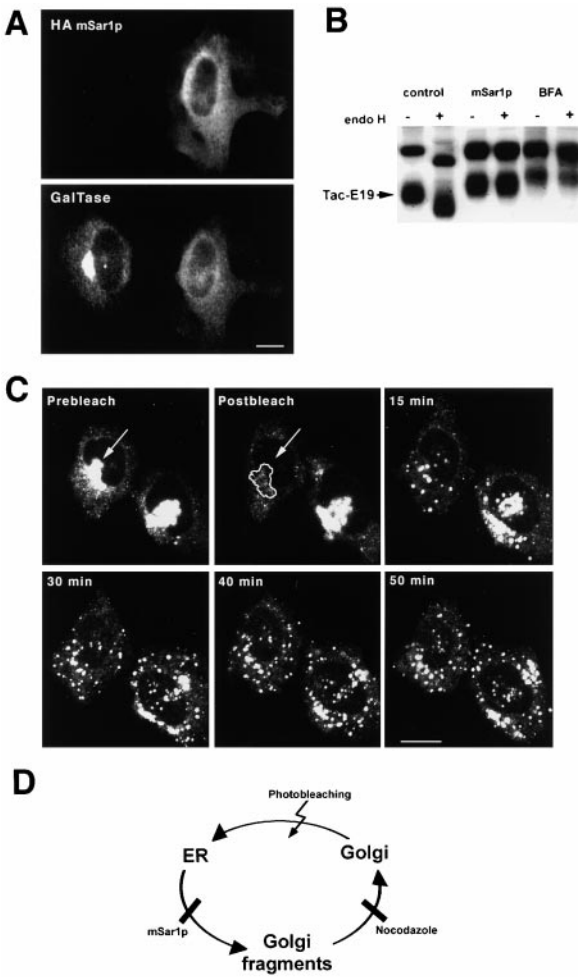

Figure 3. Blocking ER to Golgi Recycling Leads to Dispersal of Golgi Proteins

(A) Inhibition of ER exit by mSar1p leads to redistribution of Golgi proteins into the ER. HA-tagged Sar1T39N DNA (2 mg/ml) was microinjected into the nucleus of CHO cells. After 5 hr, cells were fixed and stained with antibodies to HA (to identify injected cells; upper panel) and to GalTase (lower panel). In uninjected cells, GalTase was concentrated in the juxtanuclear Golgi (cell on the left in the lower panel). By contrast, the mSar1p-injected cell had no concentrated Golgi labeling, and GalTase was dispersed throughout the cell (excluding the nucleus). Bar, 10 μm.

(B) Golgi enzymes redistributed by mSar1p or treatment with BFA process glycoproteins residing in the ER. Cells expressing the ER resident glycoprotein Tac-E19 were incubated for 8 hr after transfection with Sar1T39N DNA or were treated with BFA for 3 hr. Parallel observations on GalTase-GFP-expressing cells showed that Golgi enzymes had become redistributed by this time. In untreated cells, Tac-E19 was sensitive to endoH, migrating at a faster rate on the gel than control samples. Expression of mSar1p or treatment with BFA resulted in loss of endoH sensitivity of Tac-E19, indicating that it had been processed by Golgi enzymes.

(C) Nocodazole-induced Golgi fragments form de novo from the ER pool of GalTase-GFP. CHO cells stably expressing GalTase-GFP were treated with 1 μg/ml nocodazole to depolymerize microtubules and 10 μg/ml cycloheximide to inhibit protein synthesis. In the upper cell, the region containing the Golgi complex (arrow) was photobleached to remove most of the fluorescence from Golgi membranes. The cells were them imaged over time to follow the formation of Golgi fragments containing GalTase-GFP. Bar, 10 μm.

(D) Perturbations in different steps of ER/Golgi trafficking lead to Golgi disassembly/remodeling by a common pathway involving the ER.

into and function within the ER when ER exit is blocked by mSar1p expression.

The appearance of dispersed Golgi elements upon microtubule disruption with nocodazole (Turner and Tartakoff, 1989) has been attributed to either direct fragmentation of the Golgi (Shima et al., 1998) or trapping of recycling Golgi proteins in the intermediate compartment, which use microtubules to track toward the Golgi (Cole et al., 1996a; Storrie et al., 1998). To test these models, we analyzed the effect of nocodazole in GalTase-GFP expressing, cycloheximide-treated cells in which the fluorescent Golgi pool was bleached.

Immediately after bleaching, only diffusely distributed ER-localized GalTase-GFP was visible (Figure 3C). Within 15 min, however, numerous bright GalTase-GFP-enriched structures began to appear at scattered sites, becoming larger and brighter over time. These structures were relatively stationary in the cytoplasm and resembled in both number and distribution the dispersed Golgi elements arising in control cells. Total cellular fluorescence remained constant throughout the recovery period (data not shown), so the increased brightness in peripheral structures reflected changes in concentrations of GalTase-GFP fluorescence and not the appearance of new fluorescence. Because only one source of fluorescence (i.e., the ER) was available for generating the fluorescent peripheral structures, this demonstrates that direct fragmentation/dispersal of Golgi membranes is not required for the formation of peripheral Golgi elements in nocodazole-treated cells. Instead, Golgi protein cycling pathways involving the ER as an intermediate appear to underlie the "fragmented" Golgi phenotype.

The two perturbants we examined disrupt ER/Golgi trafficking at different steps (Figure 3D). Overexpression of mSar1p blocks ER export and traps recycling Golgi enzymes in the ER. Nocodazole treatment does not block ER export but allows Golgi enzymes that cycle through the ER to accumulate in pre-Golgi intermediates/Golgi fragments, which are unable to translocate to the perinuclear region due to the absence of microtubules. Nevertheless, both these perturbants lead to Golgi disassembly/remodeling by a common pathway involving the ER.

Visualization and Quantitation of Golgi Disassembly and Reassembly in Mitosis

The Golgi complex undergoes reversible disassembly each cell cycle during mitosis (Warren and Wickner, 1996). At the same time, forward trafficking out of the ER is blocked (Featherstone et al., 1985; Farmaki et al., 1999) and cytoplasmic microtubules are depolymerized (Wadsworth and Sloboda, 1983). Because these are conditions in interphase cells that lead to Golgi disassembly/remodeling, we asked whether similar alterations in Golgi protein cycling pathways during mitosis might underlie mitotic Golgi breakdown and reassembly. To pursue this, we examined the distribution of Golgi proteins in mitotic cells by time-lapse imaging of GalTase-GFP in several different cell types (including CHO, HeLa, PTK1, and NRK) with similar results in all cases.

Several distinct stages could be identified as Golgi membranes broke down and then reassembled in mitotic cells (Figure 4A). During early prophase, when centrosome duplication and migration to opposite poles of the nucleus occurs, the juxtanuclear Golgi ribbon seen during interphase (Figure 4A; t = 0 min) appeared to be pulled apart, with Golgi membranes wrapping around the nucleus (t = 26–34). Numerous small, nonmotile Golgi structures then began to appear throughout the cytoplasm over the course of 4–5 min (t = 36–38). Simultaneously, the perinuclear Golgi elements disappeared.

Between late prophase and early metaphase, coinciding with the loss of nuclear envelope integrity, the dispersed Golgi fragments grew fainter, and fluorescence became more diffusely distributed. At metaphase (t = 40), virtually no Golgi fragments were visible, and fluorescence was distributed throughout the cell except for areas occupied by chromosomes. Sections collected through the entire cell depth showed no large fluorescent structures anywhere in the cell (Figure 4B, see GalTase-GFP). Occasionally, small structures enriched in GalTase-GFP were observed, but the fluorescence associated with these structures was always only a minority of total fluorescence. Other Golgi markers analyzed by Z sectioning, including the Golgi enzymes mannosidase II and sialyltransferase, and the *cis*-Golgi matrix protein GM130 (Nakamura et al., 1995), also were completely dispersed in metaphase (Figure 4B). The diffuse staining pattern, therefore, is a general phenotype for Golgi membrane proteins in metaphase.

The dispersed, cell-filling fluorescence pattern of GalTase-GFP remained until cytokinesis (Figure 4A; t = 58). Then, small Golgi fragments enriched in GalTase-GFP quickly reappeared at random sites, associated with the rapid diminishment of diffuse staining. As cells flattened, the newly formed Golgi fragments translocated to the centrosomal region of each daughter cell (t = 68) and coalesced into larger Golgi structures (t = 80), eventually reforming a ribbon-like, juxtanuclear Golgi structure (t = 120).

When these changes in Golgi morphology during mitosis were quantified (Figure 4C), total cellular fluorescence was found to remain constant as GalTase-GFP changed its distribution. Approximately half of GalTase-GFP fluorescence was associated with distinct Golgi elements/fragments in prophase, with the remaining fluorescence (i.e., nonfragment) dispersed throughout the cell. As cells progressed into metaphase, Golgi fragment fluorescence rapidly declined as diffusely distributed fluorescence increased. Fragment fluorescence became negligible (less than 2% of total fluorescence) from metaphase to telophase. During cytokinesis, Golgi fragment fluorescence increased as nonfragment staining decreased until fragment fluorescence reached a similar percentage of total as observed before entry into mitosis.

The above results suggest Golgi disassembly/reassembly during mitosis can be described in terms of four progressive stages: (1) loss of the perinuclear Golgi ribbon and appearance of peripheral Golgi fragments (at prophase); (2) loss of Golgi fragments and redistribution of Golgi proteins into widely dispersed membranes (between metaphase and telophase); (3) reappearance of small peripheral Golgi fragments (during late telophase to early cytokinesis); and (4) coalescence of Golgi fragments into a juxtanuclear site (at cytokinesis).

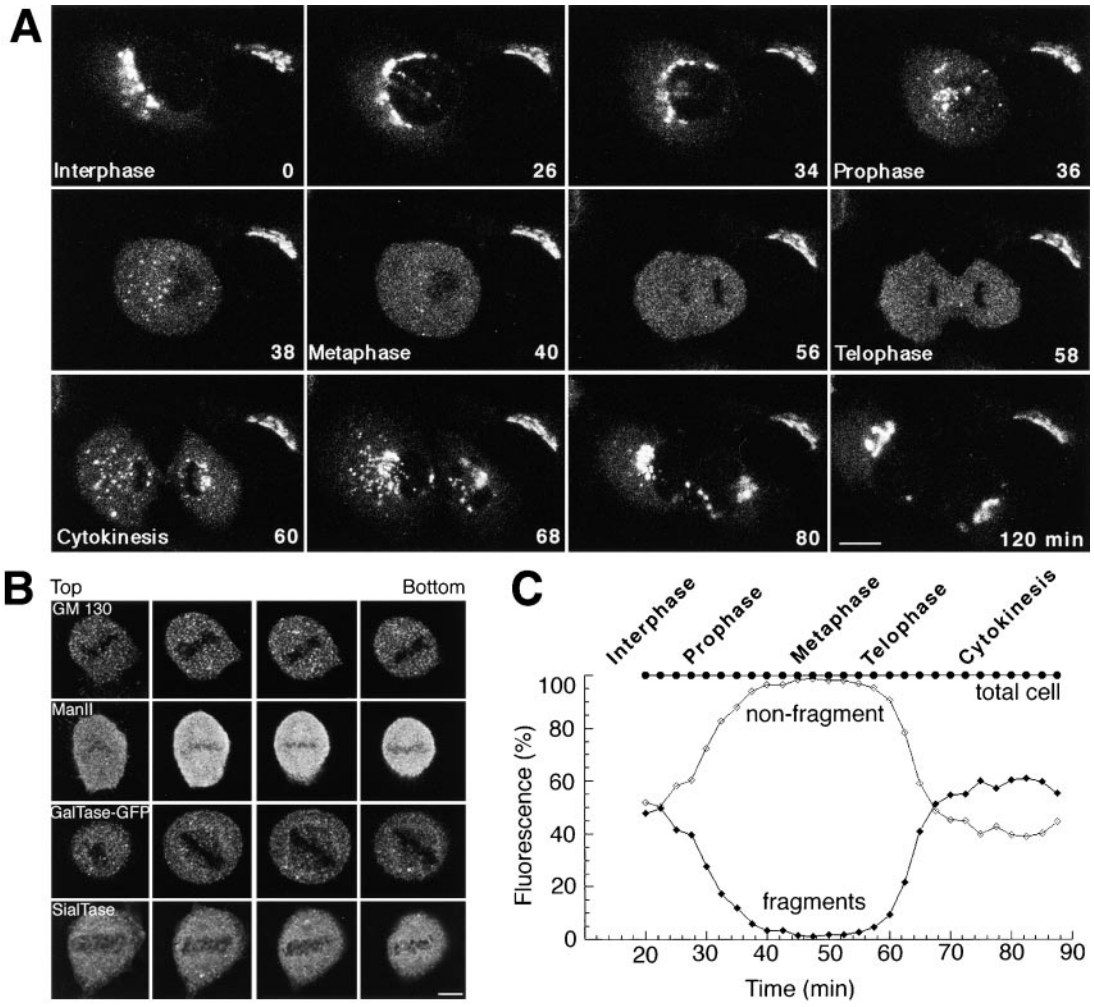

Figure 4. Dispersal of Golgi Protein during Mitosis Is a Multistep Process

(A) HeLa cells expressing GalTase-GFP were imaged with a confocal microscope. Optical sections (two planes, 2 μm spacing) were collected at 2 min intervals for 10 hr. The images show Z axis projections at representative time points. The right cell remained in interphase during the observation period, while the left cell underwent mitosis, which was accompanied by striking changes in the distribution of GalTase-GFP. Bar, 10 μm. See Quicktime movies at <http://dir.nichd.nih.gov/cbmb/pb9labob.html>.

(B) Distribution of endogenous Golgi proteins (GM130, Man II, and sialyltransferase) analyzed by Z sectioning of immunolabeled NRK cells at metaphase and in metaphase HeLa cells expressing GalTase-GFP. Bar, 10 μm.

(C) To quantify the changes in GalTase-GFP during mitosis, images of stably expressing CHO cells were collected with a 40× 1.3 NA objective and a cooled CCD camera. Fragment-associated fluorescence (see Experimental Procedures), which was about 50% of total fluorescence at the onset of mitosis, rapidly declined as cells entered metaphase. During metaphase and telophase (an interval of about 20 min), essentially all GalTase-GFP fluorescence was dispersed. After cytokinesis, fragment-associated fluorescence increased, and the fraction of fluorescence in the dispersed state declined. One hour after the beginning of mitosis, the distribution of GalTase-GFP was essentially the same as observed in interphase cells.

Localization of Golgi Proteins in ER Membranes of Mitotic Cells

The time-lapse imaging experiments above showed that Golgi proteins are dispersed throughout the entire cell during stage 2 of mitotic Golgi disassembly/reassembly, when cytoplasm is partitioned between daughter cells. To identify the compartment in which Golgi proteins reside at this stage, we examined the distribution of Golgi markers by electron microscopy. Interphase cells expressing Man II-GFP that were immunogold labeled (Figures 5A–5C) showed gold particles concentrated within juxtanuclear stacked Golgi cisternae with only occasional particles localized in ER membranes. By contrast, cells selected in stage 2 of mitotic Golgi disassembly/reassembly (Figures 5G–5I) showed gold particles predominantly associated with ER membranes, which appeared as elongated cisternae carrying bound ribosomes (Figure 5I). These results demonstrate that the stage of mitosis when Golgi proteins are widely dispersed throughout the cytoplasm represents a time when these proteins are localized within ER membranes.

Immunoperoxidase staining of native GalTase was performed to compare Golgi protein distributions at different stages of mitosis. Interphase cells showed clear labeling of the Golgi complex (Figures 5D–5F), with labeling most abundant in the 2–4 cisternae of the mid/trans part of the stack (Figure 5E). Mitotic cells (containing condensed chromatin and no nuclear envelope) showed two different patterns of labeling that represented sequential intermediates in the process of Golgi

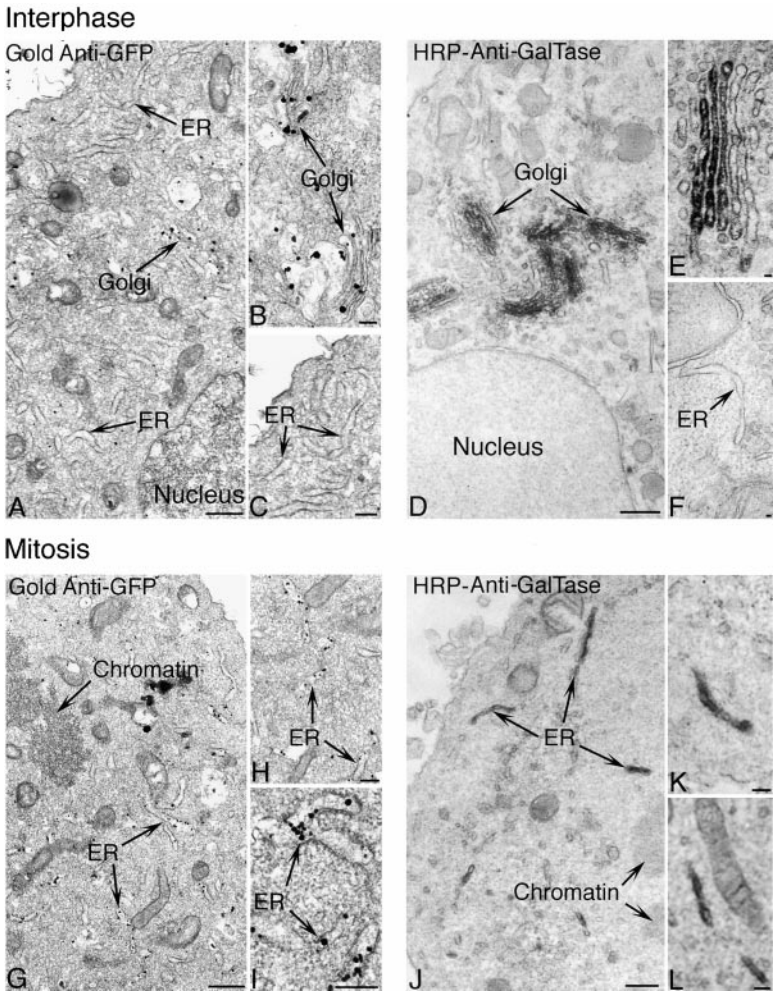

Figure 5. Ultrastructural Localization of Golgi Enzymes in Interphase and Mitotic Cells

(A) Silver-enhanced immunogold labeling of ManII-GFP in interphase NRK cells showed an enrichment of gold particles in the juxtanuclear Golgi region by electron microscopy. (B) At higher magnification, this region showed gold particles over stacked Golgi cisternae. (C) Very little gold labeling was observed within ER cisternae, which appeared as elongated cisternae carrying ribosomes.

(D) Immunoperoxidase EM labeling of native GalTase in an interphase HeLa cell. The black HRP reaction product was localized almost exclusively within stacked Golgi cisternae in the juxtanuclear region and absent from ER membranes (including the nuclear envelope). (E and F) Higher magnification of HRP labeling of native GalTase in HeLa cells shows HRP reaction product in Golgi cisternae and the lack of staining in ER cisternae.

(G) Mitotic NRK cells expressing ManII-GFP that showed a diffuse distribution of the chimera at the light microscope level were selected for ultrastructural analysis. In these cells, gold particles were predominantly localized in the lumen of ER membranes, which were elongated, carried ribosomes, and were distributed throughout the cell. Golgi particles in these cells were largely absent from other cytoplasmic structures.

(H and I) Mitotic ER membranes labeled with ManII-GFP gold particles in these cells are shown at higher magnification.

(J–L) Immunoperoxidase labeling of native GalTase in mitotic HeLa cells. HRP reaction product was observed in elongated ER cisternae distributed throughout the cell.

Bars (A, D, G, and J), 500 nm; (B, C, E, F, H, I, K, and L), 200 nm.

breakdown/reassembly. In one pattern, GalTase labeling was present predominantly in tubular-membrane clusters (0.5–2.0 μm diameter) that were localized at scattered sites in the cytoplasm (data not shown). These structures corresponded to the mitotic Golgi fragments in stages 1, 3, and 4 of Golgi disassembly/reassembly observed in our time-lapse imaging (see Figure 4A) and were reminiscent of "mitotic Golgi clusters" described by Lucocq et al. (1989) and by Acharya et al. (1998). The second pattern corresponded to cells in stage 2 of Golgi breakdown/reassembly, where Golgi proteins are diffusely distributed in the cytoplasm. In this pattern, GalTase labeling was found in ER cisternae (Figures 5J–5L) that extended as long tubules. The levels of immunoperoxidase staining in ER cisternae of these mitotic cells was similar to that in ER cisternae of BFA-treated cells (data not shown). These results, in combination with our time-lapse data, suggest that Golgi proteins transit through the ER during mitosis in a sequential process where Golgi fragments are absorbed into and then reemerge from the ER.

Diffusional Mobility of GalTase-GFP in Mitotic Membranes: Evidence against Golgi Vesicles in Mitosis

Previous work has suggested that Golgi proteins disperse into small vesicles during mitosis (Lucocq et al., 1989). Because such vesicles might have been missed using our EM approach, we probed for mitotic Golgi vesicles using fluorescence recovery after photobleaching (FRAP). We found that recovery of GalTase-GFP into a bleached box was extremely rapid and complete in cells at stage 2 of mitotic Golgi disassembly/reassembly (e.g., metaphase; Figure 6A). Quantitative FRAP experiments (Figure 6C) revealed the diffusion constant (*D*) of GalTase-GFP to be 0.28 ± 0.04 $\mu m^2/s$ with no significant immobile fraction. An identical *D* and negligible immobile fraction were found for GalTase-GFP in interphase ER membranes (Figure 6D, 0.30 ± 0.04 $\mu m^2/s$). For mitotic vesicles to give rise to these measured diffusive kinetics, Golgi proteins would have to be localized in a uniform vesicle population that coincidentally diffuses at exactly the same rate as GalTase-GFP in interphase ER. Given the improbability of this, the data favor the view that GalTase-GFP redistributes primarily into ER membranes rather than into isolated vesicles during stage 2 when GalTase-GFP fluorescence is dispersed throughout the cell.

Further evidence against a mitotic Golgi vesicle population was obtained by comparing the diffusional mobility of Golgi protein and lipid (Figure 7). If Golgi proteins redistribute into small vesicles that move freely through the cytoplasm, Golgi lipid and protein markers would be expected to recover at identical rates into a bleached

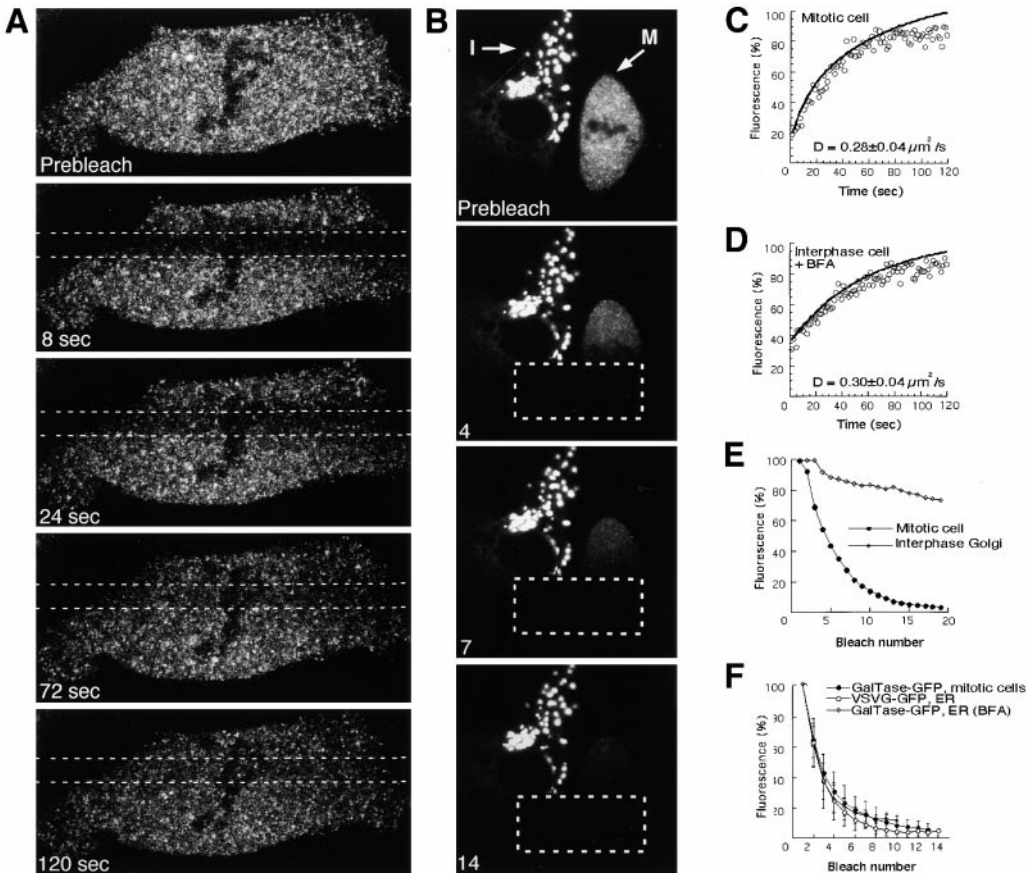

Figure 6. Diffusional Mobility of GalTase-GFP in Mitotic Cells

(A) FRAP experiment on a PTK1 cell expressing GalTase-GFP in metaphase. The area between the dashed lines was bleached through its depth by a single scan with high laser power. Recovery was monitored by scanning the entire cell at low laser power. (C and D) Quantitative analysis of diffusional mobility of GalTase-GFP in a mitotic cell (C) and an interphase cell treated with BFA to redistribute the protein from the Golgi into the ER (D). The plots show experimental data, and the curves are derived from a computer model used to calculate the diffusion coefficient *D*. The *D* values shown represent the mean of ten experiments.

(B) FLIP in GalTase-GFP-expressing PTK1 cells. A boxed area spanning part of both an interphase cell (left) and a mitotic cell (right) was repetitively photobleached (four scans, first cycle; ten scans thereafter) with high laser power. After each cycle of bleaching, an image of the cells was collected using low laser power. The numbers of bleaching cycles are indicated at the lower left corner of the images. The fluorescence intensities of the metaphase cell (M) outside the bleached region and of the Golgi elements in the interphase cell (I) are plotted against numbers of photobleach cycles in (E). (F) The rate of FLIP was compared in metaphase CHO cells and interphase CHO cells expressing GFP chimeric proteins localized in the ER (cells expressing GalTase-GFP treated with BFA, and cells expressing VSVG-GFP at 40°). Since interphase cells are typically flatter than mitotic cells, the interphase cells were trypsinized and replated to make them more equivalent in shape. In each instance, one-fifth of the diameter of the cell was repetitively bleached using identical protocols, and residual fluorescence was measured in a region outside the bleached area.

area, since they would be moving in a common vesicle carrier rather than by diffusion of individual components in a continuous bilayer system (Figure 7B). If they are both in an interconnected membrane system, lipid would be expected to move significantly faster (Edidin et al., 1994). To measure lipid diffusion, we used BODIPY ceramide, which concentrates in Golgi membranes in interphase cells (Figure 7A; Pagano et al., 1991). This staining pattern changed dramatically in mitotic cells, with the lipid marker redistributing into widely dispersed membranes, and into a few bright peripheral elements (Figure 7A). FRAP experiments of BODIPY ceramide–labeled membranes in interphase cells treated with BFA revealed *D* of the lipid to be ten times faster than *D* of GalTase-GFP in ER membranes (with no immobile fraction; Figure 7C), as expected for lipid versus protein diffusion in a bilayer. Significantly, *D* of BODIPY ceramide remained ten times faster than GalTase-GFP in mitotic membranes at metaphase (Figure 7C). The data are thus inconsistent with a vesicle redistribution model and support the idea that Golgi lipid and protein in mitotic cells at metaphase have both redistributed into the continuous bilayer system of the ER.

GalTase-GFP Diffuses throughout Metaphase ER Membranes

During mitosis, ER membranes remain as elaborate membrane networks, with little or no fragmentation or vesiculation (Ellenberg et al., 1997). To address whether GalTase-GFP in metaphase cells diffuses throughout such an interconnected system or resides in subdomains and/or separate noncontinuous compartments,

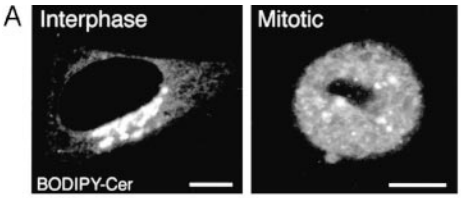

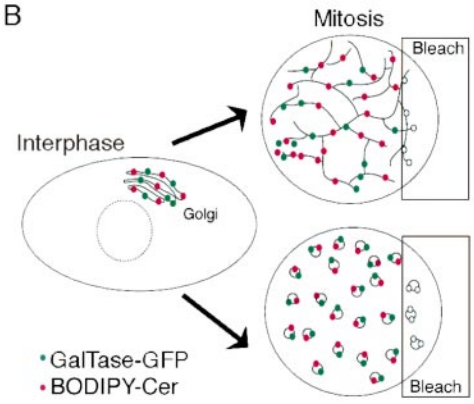

C

Cell Cycle Stage	Label	D ($\mu m^2/s$)
Interphase	GalTase-GFP	0.28 ±0.04
	BODIPY-Cer	2.0 ±0.3
Mitotic	GalTase-GFP	0.30 ±0.04
	BODIPY-Cer	2.4 ±0.3

Figure 7. During Metaphase GalTase-GFP Does Not Localize in Rapidly Moving Small Vesicles

(A) HeLa cells were labeled with 5 μM BODIPY ceramide for 10 min at 37°C, washed, and chased for 40 min to allow accumulation in the Golgi complex. BODIPY-ceramide-labeled cells in interphase and mitosis are shown. Bars, 10 μm. (B) Model of possible dispersed locations (vesicles versus ER) of Golgi components during mitosis. Results from FRAP experiments (C) revealed the diffusion coefficient, *D*, of BODIPY-ceramide was ten times faster than GalTase-GFP in both interphase and mitotic membranes, favoring the ER redistribution model.

we repetitively bleached a small area of the cell while monitoring fluorescence in other areas of the cell (Cole et al., 1996a). Rapid and almost complete loss of total cellular fluorescence was seen after ten consecutive bleaches of the rectangular box in metaphase cells at stage 2 of Golgi disassembly/reassembly (Figure 6B, right cell). By contrast, in the neighboring interphase cell, fluorescence was lost from the ER, but the Golgi elements remained bright (Figure 6B, left cell). These results are quantified in Figure 6E, where fluorescence outside the bleached region are plotted against the number of bleach cycles. No discontinuous pockets of GalTase-GFP fluorescence were observed.

The loss of fluorescence in metaphase cells followed a similar time course to that measured in repetitive bleaching experiments of interphase cells in which GalTase-GFP or VSVG-GFP were redistributed from Golgi to ER by treatment with BFA (Figure 6F). By contrast, organelles labeled by rhodamine transferrin or dextran taken up from the cell surface did not show significant loss of fluorescence by repetitive bleaching of a small area of the cell. Collectively, these results provide further evidence against a vesicle and/or fragment pool of GalTase-GFP in metaphase cells at stage 2 of Golgi disassembly/reassembly and indicate that mitotic ER membranes containing GalTase-GFP are extensively interconnected, with GalTase-GFP diffusing freely and rapidly from one region of the ER to another.

Expression of mSar1p Inhibits Formation of Golgi Stacks at Cytokinesis

If Golgi proteins are redistributed into the ER in mitotic cells, then conditions that block ER export should prevent reassembly of the Golgi complex, whereas they would not be expected to affect Golgi reassembly from a vesicle population. To test this, we microinjected low concentrations of mSar1p DNA into cells. Following a short incubation to allow expression of mSar1p, we then analyzed the distribution of native GalTase.

Because the cells were not synchronized in these experiments, mSar1p-expressing cells at all stages of the cell cycle were observed (Figures 8A–8C). Interphase cells had largely intact Golgi structures, indicating that the period of expression of mSar1p was not long enough to trap recycling Golgi proteins in the ER (Figure 8C). However, Golgi reassembly at cytokinesis was inhibited in mSar1p-expressing cells, with Golgi proteins remaining widely dispersed throughout the cell (Figure 8C, arrows). This contrasted with noninjected cells at cytokinesis where most of GalTase was concentrated within numerous emerging Golgi fragments (Figure 8D). These results indicate that export of Golgi proteins from the ER is essential for the reformation of the Golgi complex after mitosis (Figure 8E).

Discussion

The existence of Golgi-ER recycling pathways has been recognized for many years, but their significance for Golgi biogenesis and maintenance has not been fully appreciated. We have applied quantitative imaging and photobleaching techniques to measure the kinetics of Golgi protein recycling between the Golgi and ER in interphase cells and to monitor the dissolution and reformation of the Golgi complex during mitosis. Our findings show that the Golgi complex exists as a steady-state system in interphase cells, with rapid and substantial recycling of Golgi proteins through the ER. At all times, a significant fraction of Golgi resident proteins reside in the ER, available for export into pre-Golgi elements that subsequently become part of the Golgi complex. Maintenance of the Golgi complex thus depends on continual membrane export from the ER. During mitosis, when export from the ER stops, Golgi proteins cycle back to the ER where they become trapped. When ER egress resumes at the end of mitosis, Golgi stacks reform as Golgi proteins are exported out of the ER. The latter findings help to resolve a long-standing debate concerning the localization of Golgi components in mitotic cells and the mechanism of Golgi partitioning into daughter cells. The Golgi disperses and reforms through the intermediary of the ER, exploiting constitutive cycling pathways that also underlie the maintenance of Golgi structure in interphase cells.

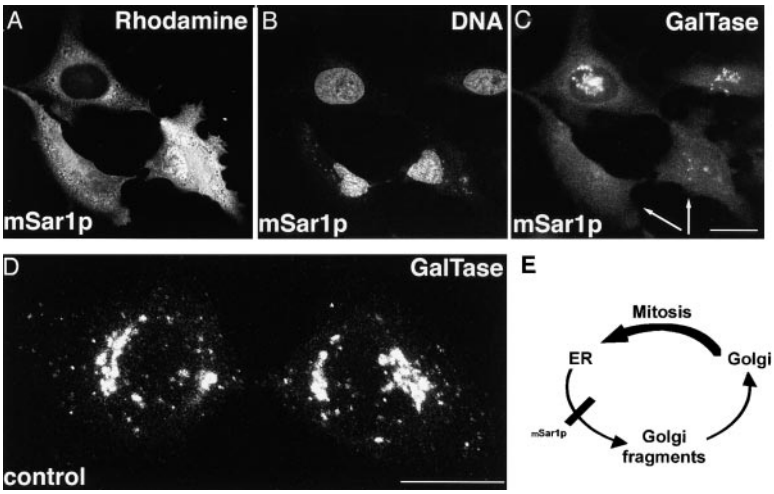

Figure 8. Block of ER Exit by Mutant Sar1p Prevents Reformation of Golgi Stacks after Mitosis

Sar1T39N plasmid (0.5 mg/ml) mixed with rhodamine dextran (70 kDa) was microinjected into HeLa cells. Cells were fixed 4 hr after injection and stained with antibodies to GalTase and Hoechst. Microinjected cells (identified by the rhodamine stain [A]) that just completed mitosis (see decondensing chromosomes in irregular shaped nuclei [B]) were analyzed for the presence of Golgi stacks containing GalTase in a projection of a series of images in the z-axis (C). Interphase cells expressing the mutated protein still had intact Golgi structures (complete dispersal of the Golgi was observed only at later time points). By contrast, cells expressing mSar1p in cytokinesis (indicated by arrows) failed to reform bright Golgi elements at times when control cells in cytokinesis had done so (D) (also see Figure 4; t = 60–120 min). (E) At the onset of mitosis, enhanced retrograde transport redistributes Golgi membranes into the ER. Export of proteins from the ER is essential for the reformation of the Golgi complex during cytokinesis. Bars, 10 μm.

Constitutive Cycling of GalTase-GFP between Golgi and ER

GalTase-GFP behaved as a bona fide Golgi resident protein in cells. Nevertheless, in single living cells the fluorescence intensity of GalTase-GFP in the Golgi complex amounted to only 70% of total cellular fluorescence. The remaining 30% came from GalTase-GFP that was distributed throughout the ER. Cells actively maintained the Golgi and ER pools of GalTase-GFP; the pool sizes remained constant when protein synthesis was inhibited and did not depend on expression level. Selective photobleaching of Golgi or ER pools of GalTase-GFP and monitoring of recovery from the nonbleached pool indicated that the steady-state concentrations in Golgi and ER membranes arose by continuous cycling rather than by GalTase-GFP residing stably within these compartments.

Kinetic modeling of the FRAP experiments revealed the rate of GalTase-GFP cycling between Golgi and ER membranes. An average GalTase-GFP molecule cycled between Golgi and ER every 85 min, residing in the Golgi for approximately 58 min and the ER for 27 min. Interestingly, the forward rate constant of GalTase-GFP (i.e., 3.6% per min) is very close to that obtained for VSVG-GFP (Hirschberg et al., 1998). This raises the possibility that the rate-limiting steps of export out of the ER for prototype Golgi resident and cargo proteins are similar.

Perturbations in Golgi Protein Cycling Lead to Golgi Remodeling/Dissolution in Interphase Cells

To test whether the bulk of Golgi membrane components constitutively recycle through the ER, we examined whether Golgi integrity was dependent on membrane export from the ER. Blocking ER export by overexpression of mSar1p caused Golgi structures to disappear, as previously reported (Storrie et al., 1998), and resulted in Golgi protein accumulation and function in the ER. Selective bleaching of Golgi fluorescence further demonstrated that the appearance of Golgi fragments in cells without microtubules results from perturbation of constitutive protein cycling pathways between Golgi and ER, and not direct fragmentation of the Golgi (Cole et al., 1996a; Storrie et al., 1998). In the absence of microtubules, Golgi proteins that have cycled back to the ER are exported into pre-Golgi elements that subsequently fail to translocate to, and become part of, the perinuclear Golgi complex.

The above results suggest that protein cycling pathways between the Golgi and ER play a fundamental role in the maintenance of Golgi integrity with the very existence of the Golgi complex a product of these pathways. That Golgi structures can form de novo from Golgi components returned to the ER is supported by experiments involving BFA washout or microsurgical removal of Golgi structures where biogenesis of the Golgi from the ER is observed (Lippincott-Schwartz et al., 1990; Maniotis and Schliwa, 1991). By existing as a steady-state system with rapid and substantial exchange of its components through the ER, the Golgi can continuously remodel itself and thereby respond to changing cellular needs.

Golgi Breakdown/Reassembly during Mitosis

The traditional model of Golgi disassembly/reassembly during mitosis postulates a direct breakdown of the Golgi complex by a process of continual budding and inhibited fusion (Warren, 1993). According to this view, Golgi enzymes enter small vesicles/clusters that persist throughout mitosis. The recreation of Golgi stacks at the end of mitosis is attributed to a mechanism by which these vesicles/clusters fuse together after their partitioning into daughter cells (Lucocq and Warren, 1987; Shima et al., 1998).

Evidence from previous work and the present study, however, indicates that during mitosis similar conditions arise that in interphase cells lead to Golgi dissolution/fragmentation by alterations in Golgi protein cycling pathways, such as the inhibition of forward trafficking out of the ER and depolymerization of cytoplasmic microtubules (Featherstone et al., 1985; Zhai et al., 1996). We therefore asked whether Golgi-ER cycling pathways play analogous roles in Golgi disassembly and reformation in mitosis to those they play in interphase. To address this, we visualized Golgi disassembly/reassembly

during mitosis by fluorescence time-lapse imaging and found that mitotic Golgi breakdown/reassembly progresses through a series of stages, within which the ER plays an intermediary role.

The first stage observed was the disappearance of the perinuclear Golgi ribbon and the appearance of numerous, smaller, peripheral elements. This occurred at prophase, when cytoplasmic microtubules undergo disassembly. Some of the peripheral Golgi elements may have arisen by subdivision and transport from the perinuclear Golgi complex. However, others are likely to have formed de novo by export from the ER, since centripetal movement of Golgi elements was not seen. The formation of these mitotic peripheral Golgi structures thus would be analogous to the formation of peripheral Golgi elements observed in cells with microtubules depolymerized by nocodazole treatment (Cole et al., 1996a; Storrie et al., 1998).

The second stage was characterized by the dramatic disappearance of Golgi elements and the redistribution of Golgi proteins into widely dispersed membranes from metaphase through telophase. Previous work has shown that protein export from the ER is blocked at this time (Featherstone et al., 1985; Farmaki et al., 1999), raising the possibility that the diffuse Golgi protein distribution represents proteins trapped in the ER. Quantitation showed that more than 90% of GalTase-GFP was dispersed throughout the cell at this stage, with very little, if any, fluorescence in discrete Golgi structures. Other Golgi proteins detected by immunolabeling, including mannosidase II, sialyltransferase, GM130, and GalTase, became similarly dispersed in metaphase/telophase. There are reports that Golgi proteins reside predominantly within numerous Golgi fragments throughout mitosis (Shima et al., 1998), but the percentage of total fluorescence residing in these fragments was not reported. The quantitative observations described in this paper indicate that the bulk of Golgi proteins are in a dispersed state in metaphase/telophase and not in Golgi fragments.

The diffuse, cell-filling fluorescence pattern of Golgi proteins (i.e., stage 2) lasted until cytokinesis, when small Golgi fragments enriched in GalTase-GFP then began to appear at peripheral sites. Their appearance correlated with the diminishment of diffuse staining. This represented the third stage of mitotic Golgi disassembly/reassembly, when protein export from the ER resumes (Souter et al., 1993). In the fourth and final stage, the Golgi fragments clustered toward the centrosomal region of each daughter cell, reforming the juxtanuclear Golgi ribbon. The directed, inward movement of Golgi fragments at this stage is likely to be mediated by microtubules (Shima et al., 1998), since cytoplasmic microtubules are repolymerized and emanate out from the centrosomal region during late cytokinesis.

Evidence for an ER Localization of Golgi Proteins in Mitotic Cells

Previous ultrastructural and biochemical studies have proposed three different localizations for Golgi proteins upon mitotic disassembly of the Golgi complex: dispersed vesicles, vesicle clusters/fragments, and the ER (Lucocq et al., 1989; Thyberg and Moskalewski, 1992; Jesch and Linstedt, 1998; Shima et al., 1998). Our time-lapse observations help explain these disparate results by showing that Golgi proteins reside in fragments at certain stages of mitosis (i.e., stages 1, 3, and 4). However, at the critical stage (i.e., stage 2) when the Golgi partitions between daughter cells, Golgi proteins are highly dispersed throughout the cell within ER membranes.

Localization of Golgi proteins within the ER during stage 2 of mitotic disassembly/reassembly was demonstrated by electron microscopy of immunogold-labeled mitotic cells specifically selected at this stage. Photobleaching experiments ruled out the possibility that, in addition to ER, a population of Golgi proteins at this stage resided in vesicles. Greater than 95% of GalTase-GFP at this stage of mitosis exhibited movement that was quantitatively diffusive (in all directions) and was not driven by an active mechanism (e.g., by actin or microtubules). The calculated *D* was identical to GalTase-GFP in interphase ER membranes. A Golgi lipid marker, BODIPY ceramide, in mitotic cells exhibited a *D* that was ten times higher than GalTase-GFP, ruling out that the two resided in a common vesicle carrier, and consistent with their diffusing within a common bilayer system where lipid diffuses much faster than protein. Repetitive bleaching experiments, furthermore, revealed that, like ER, mitotic membranes containing GalTase-GFP were extensively interconnected. Finally, reformation of Golgi structures at cytokinesis was inhibited by mutant Sar1p, which blocks ER export. Collectively, these findings indicate that Golgi proteins at metaphase/telophase reside primarily within ER membranes instead of isolated vesicles/clusters.

Potential Mechanisms Underlying Mitotic Golgi Disassembly/Reassembly

The finding that export of proteins from the ER is blocked in mitosis (Featherstone et al., 1985) at the early stage of COPII-mediated budding (Farmaki et al., 1999) raises the possibility that Golgi proteins redistribute into the ER during mitosis by being trapped in this compartment during constitutive recycling. However, the basal rate of retrograde GalTase-GFP trafficking in interphase cells (Figure 2D) was far too slow to account for the rapid decline in Golgi fragment–associated fluorescence seen at the onset of mitosis (Figure 4C). Indeed, some regulatory mechanism must accelerate retrograde traffic by at least 20-fold, even if it is assumed that anterograde traffic comes to a complete standstill. In interphase cells, several conditions can cause enhanced retrograde traffic to the ER. Treatment of cells with BFA, which inhibits nucleotide exchange onto ARF (Peyroche et al., 1999), leads to loss of ARF and COPI binding to membranes (Donaldson et al., 1991) and rapid fusion of Golgi structures with the ER (Sciaky et al., 1997). Other examples of enhanced retrograde traffic to the ER include osmotically induced cell volume changes (Lee and Linstedt, 1999) and overexpression of KDELR (Hsu et al., 1992). It is possible, therefore, that some component(s) in mitotic cytoplasm activates a similar mechanism(s) that causes retrograde traffic to accelerate at the time ER export is inhibited. The machinery and signaling pathways leading to mitotic Golgi disassembly/reformation have only just begun to be delineated (Acharya et

al., 1998; Lowe et al., 1998; Farmaki et al., 1999). How alterations in these mechanisms lead to inhibition of ER export and stimulation of retrograde traffic during mitosis, therefore, will be important questions to address in future work aimed at understanding mitotic Golgi disassembly/reassembly.

Experimental Procedures

DNA Constructs and Cell Transfection

A triple GFP concatamer was constructed in pEGFP-N1 (Clontech Laboratories, Palo Alto, CA). GalTase from GalTase-GFPS65T and ManII from ManII-GFP (Cole et al., 1996b) were subcloned into this vector. VSVG-GFP and Tac-E19 constructs were as described in Presley et al. (1997) and Hsu et al. (1992), respectively. Sar1T39N (mSar1p) DNA (from O. Kuge) was HA-tagged and cloned into pTarget (Promega, Madison, WI). Cells were transfected transiently by electroporation (using 10 μg DNA) or by microinjection, using 0.5 μg/ml DNA (for mitotic studies) or 2 μg/ml DNA (for interphase studies; described in Ellenberg et al., 1997).

Cells and Reagents

The following antibodies were used: polyclonal antibodies to GM130 (from G. Warren); polyclonal anti-galactosyltransferase (from E. G. Berger); polyclonal ER antiserum (from D. Louvard); monoclonal anti-ManII (from K. Moreman); polyclonal anti-sialyltransferase (from K. J. Colley); fluorescently labeled secondaries from Southern Biotechnology (Birmingham, AL); and polyclonal anti-GFP antibody from Clontech Laboratories. Brefeldin A, used at 1 μg/ml, was from Epicentre Technologies (Madison, WI). Nocodazole (1 μg/ml) and cycloheximide (10 μg/ml) were from Sigma Chemical Co. (St. Louis, MO). Hoechst 33342 (Molecular Probes, Eugene, OR) was used at 0.08 μg/ml. BODIPY ceramide (Molecular Probes, Eugene, OR) was used as described in Sciaky et al. (1997).

Immunofluorescence and Electron Microscopy

Cells were prepared for immunofluorescence microscopy as described previously (Sciaky et al., 1997). For immunogold labeling, cells were fixed for 2 min in 2% acrolein and 2% paraformaldehyde in 0.1 M phosphate buffer, incubated in blocking buffer containing 5% normal goat serum (NGS) and 0.1% saponin in PBS for 1 hr. Cells were then incubated with anti-GFP antibody at 1:1000 for 1 hr and then rinsed in PBS containing 1% NGS. Subsequently cells were incubated with 1.4 nm Nanogold conjugated secondary antibody at 1:200 (Nanoprobes, Stonybrook, NY) for 1 hr, washed, and incubated in 2% glutaraldehyde in PBS for 30 min. Cells were then treated with standard silver enhancement (HQ kit, Nanoprobes) for 6 min, incubated in 0.2% OsO_4 in 0.1 M phosphate buffer for 30 min, and further processed as described (Tanner et al., 1996). Cells for immunoperoxidase histochemistry were synchronized with an aphidicolin block (5 μg/ml for 24 hr), released for 10 hr, and prepared for EM (Polishchuk et al., 1999).

Image Acquisition and Analysis

Confocal microscope images were captured on a LSM 410 or LSM 510 (Zeiss) using 488 nm laser excitation for GFP, 568 nm for rhodamine, and 351 nm for Hoechst dye. Images for illustrations and for 3D reconstruction were captured with a 63× 1.4 NA objective using a pinhole diameter equivalent to one to two times the Airy disk diameter.

Images for quantitation of Golgi- and non-Golgi-associated fluorescence were captured with a 40× 1.3 NA objective and an open pinhole to collect fluorescence from the entire depth of the cell. Contrast and black level were adjusted such that all intensity values were within the measurable range (0 to 255 gray levels). The images were analyzed with NIH Image software (W. Rasband, NIH, Bethesda, MD). Pixel values were corrected for noncellular background. Golgi fluorescence was measured within a region that included the entire juxtanuclear Golgi complex, and the fluorescence located in non-Golgi structures was calculated by subtracting Golgi fluorescence from total cell fluorescence. GalTase-GFP fluorescence did not change upon redistribution from Golgi to ER within these cells.

Time-lapse sequences of images of mitotic cells were captured on a LSM 410. Two optical sections (2 μm spacing) were collected at each time point and subsequently projected using maximum projection.

Time-lapse images used for quantitation of fluorescence at different stages of the mitosis were acquired with a 40× 1.3 NA objective on a custom-built microscope (Presley et al., 1997). To quantitate fluorescence associated with Golgi fragments, images were background subtracted and then thresholded using a threshold value chosen to exclude diffuse staining at its maximum (in metaphase). All pixels above the threshold were considered part of Golgi fragments. On the images analyzed, our definition of Golgi fragments corresponded closely to Golgi fragments determined by visual inspection.

Photobleaching Recovery Studies and Kinetic Modeling

Selective bleaching of the Golgi and ER was performed on a LSM 510. For quantitation of fluorescence, two pseudosimultaneous images were captured, one acquired with low intensity illumination (5% transmittance) and the other with moderate intensity illumination (30% transmittance). After images recording the initial fluorescence distributions were captured, fluorescence in a selected region was bleached by scanning the region with high intensity illumination (100% transmittance). Recovery was monitored at 5 min intervals thereafter. Quantitation of fluorescence was performed on the 5% transmission images, in which all intensity values were within the measurable range. Images acquired with 30% transmission were used for illustrations. Analysis of FRAP and FLIP experiments was performed as described in Lippincott-Schwartz et al. (1998).

To quantify the interphase rates of anterograde and retrograde trafficking between ER and Golgi compartments, standard methods of kinetic analysis (Jacquez, 1996) and SAAMII software was used (Foster et al., 1994). Coefficients of variation for the rate constant estimates were both near 10%. Mean residence times were calculated as the reciprocals of these rate constants.

For detailed experimental procedures, see <http://dir.nichd.nih.gov/cbmb/pb9labob.html>.

Acknowledgments

We thank Dr. J. Bonifacino, Dr. J. Donaldson, Dr. B. Nichols, and Dr. A. Kenworthy (NIH, Bethesda, MD) for valuable comments on this manuscript. E. S. is supported by R01 GM59018-01 from NIH. We also thank Dr. S. Tao Cheng and the staff of the NINDS EM Facility for immuno-EM analysis, and L. M. Hartnell (CBMB, NIH) for helpful contributions. We also thank those who provided reagents.

Received May 18, 1999; revised November 2, 1999.

References

Acharya, U., Mallabiabarrena, A., Acharya, J.K., and Malhotra, V. (1998). Signaling via mitogen-activated protein kinase kinase (MEK1) is required for Golgi fragmentation during mitosis. Cell *92*, 183–192.

Barlowe, C., Orci, L., Yeung, T., Hosobuchi, M., Hamamoto, S., Salama, N., Rexach, M.F., Ravazzola, M., Amherdt, M., and Schekman, R. (1994). COPII: a membrane coat formed by Sec proteins that drive vesicle budding from the endoplasmic reticulum. Cell *77*, 895–907.

Brands, R., Snider, M.D., Hino, Y., Park, S.S., Gelboin, H.V., and Rothman, J.E. (1985). Retention of membrane proteins by the endoplasmic reticulum. J. Cell Biol. *101*, 1724–1732.

Cole, N.B., Sciaky, N., Marotta, A., Song, J., and Lippincott-Schwartz, J. (1996a). Golgi dispersal during microtubule disruption: regeneration of Golgi stacks at peripheral endoplasmic reticulum exit sites. Mol. Biol. Cell *7*, 631–650.

Cole, N.B., Smith, C.L., Sciaky, N., Terasaki, M., Edidin, M., and Lippincott-Schwartz, J. (1996b). Diffusional mobility of Golgi proteins in membranes of living cells. Science *273*, 797–801.

Cole, N.B., Ellenberg, J., Song, J., DiEuliis, D., and Lippincott-Schwartz, J. (1998). Retrograde transport of Golgi-localized proteins to the ER. J. Cell Biol. *140*, 1–15.

Dascher, C., and Balch, W.E. (1994). Dominant inhibitory mutants

of ARF1 block endoplasmic reticulum to Golgi transport and trigger disassembly of the Golgi apparatus. J. Biol. Chem. *269*, 1437–1448.

Donaldson, J.G., Kahn, R.A., Lippincott-Schwartz, J., and Klausner, R.D. (1991). Binding of ARF and b-COP to Golgi membranes: possible regulation by a trimeric G protein. Science *254*, 1197–1199.

Edidin, M. (1994). Mobility and Proximity in Biological Membranes. Damjanovich, Edidin, Szollosi, and Tron, eds. (Boca Raton, FL: CRC Press), pp. 109–135.

Ellenberg, J., Siggia, E., Moreira, J., Smith, C., Presley, J., Worman, H., and Lippincott-Schwartz, J. (1997). Nuclear membrane dynamics and reassembly in living cells: targeting of an inner nuclear membrane protein in interphase and mitosis. J. Cell Biol. *138*, 1193–1206.

Farmaki, T., Ponnambalam, S., Prescott, A.R., Clausen, H., Tang, B.L., Hong, W., and Lucocq, J.M. (1999). Forward and retrograde trafficking in mitotic animal cells. J. Cell Sci. *112*, 589–600.

Featherstone, C., Griffiths, G., and Warren, G. (1985). Newly synthesized G protein of vesicular stomatitis virus is not transported to the Golgi complex in mitotic cells. J. Cell Biol. *101*, 2036–2046.

Foster, D.M., Barrett, P.H.R., Bell, B.M., Beltz, W.F., Cobelli, C., Golde, H., Jacquez, J.A., and Phair, R.D. (1994). SaamII: simulation, analysis and modeling software. BMES Bull. *18*, 19–21.

Griffiths, G., Warren, G., Quinn, P., Mathieu-Costello, O., and Hoppeler, H. (1984). Density of newly synthesized plasma membrane proteins in intracellular membranes. I. Stereological studies. J. Cell Biol. *98*, 2133–2141.

Harris, S.L., and Waters, M.G. (1996). Localization of a yeast early Golgi mannosyltransferase, Och1p, involves retrograde transport. J. Cell Biol. *132*, 985–998.

Hirschberg, K., Miller, C.M., Ellenberg, J., Presley, J.F., Siggia, E.D., Phair, R.D., and Lippincott-Schwartz, J. (1998). Kinetic analysis of secretory protein traffic and characterization of Golgi to plasma membrane transport intermediates in living cells. J. Cell Biol. *143*, 1485–1503.

Hsu, V.W., Shaw, N., and Klausner, R.D. (1992). A brefeldin A-like phenotype is induced by overexpression of a human ERD-2-like protein, ELP-1. Cell *69*, 625–635.

Jacquez, J.A. (1996). Compartmental Analysis in Biology and Medicine, Third Edition (Ann Arbor, MI: Biomedware Inc.).

Jesch, S.A., and Linstedt, A.D. (1998). The Golgi and endoplasmic reticulum remain independent during mitosis in HeLa cells. Mol. Biol. Cell *9*, 623–635.

Kuge, O., Dascher, C., Orci, L., Rowe, T., Amherdt, M., Plutner, H., Ravazzola, M., Tanigawa, G., Rothman, J.E., and Balch, W.E. (1994). Endo H1 promotes vesicle budding from the endoplasmic reticulum but not Golgi compartments. J. Cell Biol. *125*, 51–65.

Lee, T.H., and Linstedt, A.D. (1999). Osmotically induced cell volume changes alter anterograde and retrograde transport, Golgi structure, and COPI dissociation. Mol. Biol. Cell *10*, 1445–1462.

Lippincott-Schwartz, J., Donaldson, J.G., Schweizer, A., Berger, E.G., Hauri, H.P., Yuan, L.C., and Klausner, R.D. (1990). Microtubule-dependent retrograde transport of proteins into the ER in the presence of brefeldin A suggests an ER recycling pathway. Cell *60*, 821–836.

Love, H.D., Lin, C.C., Short, C.S., and Ostermann, J. (1998). Isolation of functional Golgi-derived vesicles with a possible role in retrograde transport. J. Cell Biol. *140*, 541–551.

Lowe, M., Rabouille, C., Nakamura, N., Watson, R., Jackman, M., Jämsä, E., Rahman, D., Pappin, D.J., and Warren, G. (1998). Cdc2 kinase directly phosphorylates the cis-Golgi matrix protein GM130 and is required for Golgi fragmentation in mitosis. Cell *94*, 783–793.

Lucocq, J. (1992). Mimicking mitotic Golgi disassembly using okadaic acid. J. Cell Sci. *103*, 875–880.

Lucocq, J.M., and Warren, G. (1987). Fragmentation and partitioning of the Golgi apparatus during mitosis in HeLa cells. EMBO J. *6*, 3239–3246.

Lucocq, J.M., Berger, E.G., and Warren, G. (1989). Mitotic Golgi fragments in HeLa cells and their role in the reassembly pathway. J. Cell Biol. *109*, 463–474.

Maniotis, A., and Schliwa, M. (1991). Microsurgical removal of centrosomes blocks cell reproduction and centriole generation in BSC-1 cells. Cell *67*, 495–504.

Nakamura, N., Rabouille, C., Watson, R., Nilsson, T., Hui, N., Slusarewicz, P., Kreis, T.E., and Warren, G. (1995). Characterization of a cis-Golgi matrix protein, GM130. J. Cell Biol. *131*, 1715–1726.

Pagano, R.E., Martin, O.C., Kang, H.C., and Haugland, R.P. (1991). A novel fluorescent ceramide analogue for studying membrane traffic in animal cells: accumulation at the Golgi apparatus results in altered spectral properties of the sphingolipid precursor. J. Cell Biol. *113*, 1267–1279.

Pelham, H.R.B. (1995). Sorting and retrieval between the endoplasmic reticulum and Golgi apparatus. Curr. Opin. Cell Biol. *7*, 530–535.

Peyroche, A., Antonny, B., Robineau, S., Acker, J., Cherfils, J., and Jackson, C.L. (1999). Brefeldin A acts to stabilize an abortive ARF-GDP-Sec7 domain protein complex: involvement of specific residues of the Sec7 domain. Mol. Cell *3*, 275–285.

Polishchuk, R.S., Polishchuk, E.V., and Mironov, A.A. (1999). Coalescence of Golgi fragments in microtubule-deprived living cells. Eur. J. Cell Biol. *78*, 170–185.

Presley, J.F., Cole, N.B., Schroer, T.A., Hirschberg, K., Zaal, K.J., and Lippincott-Schwartz, J. (1997). ER-to-Golgi transport visualized in living cells. Nature *389*, 81–85.

Sciaky, N., Presley, J., Smith, C., Zaal, K.J.M., Cole, N., Moreira, J.E., Terasaki, M., Siggia, E., and Lippincott-Schwartz, J. (1997). Golgi tubule traffic and the effects of brefeldin A visualized in living cells. J. Cell Biol. *139*, 1137–1155.

Shima, D.T., Cabrera-Poch, N., Pepperkok, R., and Warren, G. (1998). An ordered inheritance strategy for the Golgi apparatus: visualization of mitotic disassembly reveals a role for the mitotic spindle. J. Cell Biol. *141*, 955–966.

Souter, E., Pypaert, M., and Warren, G. (1993). The Golgi stack reassembles during telophase before arrival of proteins transported from the endoplasmic reticulum. J. Cell Biol., *122*, 533–540.

Storrie, B., White, J., Röttger, S., Stelzer, E.H.K., Suganuma, T., and Nilsson, T. (1998). Recycling of Golgi-resident glycosyltransferases through the ER reveals a novel pathway and provides an explanation for nocodazole-induced Golgi scattering. J. Cell Biol. *143*, 1505–1521.

Takizawa, P.A., Yucel, J.K., Veit, B., Faulkner, D.J., Deerinck, T., Soto, G., Ellisman, M., and Malhotra, V. (1993). Complete vesiculation of Golgi membranes and inhibition of protein transport by a novel sea sponge metabolite, ilimaquinone. Cell *73*, 1079–1090.

Tanner, V.A., Ploug, T., and Tao-Cheng, J.T. (1996). Subcellular localization of SV2 and other secretory vesicle components in PC1 cells by an efficient method of preembedding EM immunocytochemistry for cell cultures. J. Histochem. Cytochem. *44*, 1481–1488.

Thyberg, J., and Moskalewski, S. (1992). Reorganization of the Golgi complex in association with mitosis: redistribution of mannosidase II to the endoplasmic reticulum and the effects of brefeldin A. J. Submicrosc. Cytol. Pathol. *24*, 495–508.

Turner, J.R., and Tartakoff, A.M. (1989). The response of the Golgi complex to microtubule alterations: the roles of metabolic energy and membrane traffic in Golgi complex organization. J. Cell Biol. *109*, 2081–2088.

Wadsworth P., and Sloboda, R.D. (1983). Microinjection of fluorescent tubulin into dividing sea urchin cells. J. Cell Biol. *97*, 1249–1254.

Warren, G. (1993). Membrane partitioning during cell division. Annu. Rev. Biochem. *62*, 323–348.

Warren, G., and Wickner, W. (1996). Organelle inheritance. Cell *84*, 395–400.

Wieland, F.T., Gleason, M.L., Serafini, T.A., and Rothman, J.E. (1987). The rate of bulk flow from the endoplasmic reticulum to the cell surface. Cell *50*, 289–300.

Wooding, S., and Pelham, H.R.B. (1998). The dynamics of Golgi protein traffic visualized in living yeast cells. Mol. Biol. Cell. *9*, 2667–2680.

Zhai, Y., Kronebusch, P.J., Simon, P.M., and Borisy, G.G. (1996). Microtubule dynamics at the G2/M transition: abrupt breakdown of cytoplasmic microtubules at nuclear envelope breakdown and implications for spindle morphogenesis. J. Cell Biol. *135*, 201–214.